

# A Combined Fit of X-ray/Neutron Total Scattering, EXAFS, and Electron Diffuse Scattering in *RMCPProfile*: User Manual

Victor Krayzman and Igor Levin

Ceramics Division, National Institute of Standards and Technology,  
Gaithersburg MD 20899

## 1. General Info

Local-structure scattering refinements using a simultaneous fit of x-ray/neutron total scattering, EXAFS, and diffuse scattering in electron diffraction are implemented as an extension to the *RMCPProfile* software **Version 6**. Users should refer to the main *RMCPProfile* manual for this version for details regarding RMC refinements using total scattering data alone. A user is expected to have a reasonable knowledge of EXAFS phenomena and be experienced in conventional EXAFS local-structure refinements. Relevant information, including tutorials, can be found at <http://cars9.uchicago.edu/~ravel/software/>. Likewise, a reasonable knowledge of electron diffraction is required.

The present software enables accurate EXAFS calculations for large atomic configurations with both single- and multiple-scattering of a photoelectron taken into account. The number of datasets is specified in the main input **\*.dat** file used by the *RMCPProfile* (asterisk refers to the stem filename). EXAFS data can be fitted either in  $k$ - or in  $r$ -space; the choice should be specified in the **\*.dat** file. EXAFS signal is calculated for an atomic configuration described in the **\*.cfg** file. All non-structural parameters that enter the EXAFS equation, such as scattering amplitudes and phase shifts, are calculated prior to refinements using the FEFF software (<http://leonardo.phys.washington.edu/feff/>). We strongly recommend self-consistent calculations of the cluster potential implemented in the FEFF8 version. The Artemis package (<http://cars9.uchicago.edu/~ravel/software/>) can be used to evaluate photoelectron scattering paths and to perform preliminary fitting of EXAFS data. A free version of FEFF included with Artemis does not support self-consistent calculations; therefore, a user needs to import the output files from FEFF8 into Artemis manually.

Once the EXAFS option is selected in the **\*.dat** file, *RMCPProfile* will calculate an EXAFS signal for each absorber type. The calculations are carried out as a sum over signals generated for the single-, double- and triple-scattering paths having effective path lengths  $r_{\text{eff}} \leq R_{\text{max}}$ . During refinements, after each atomic move, EXAFS is re-calculated for all absorbers within the distance  $R_{\text{max}}$  from the moved atom. A list of absorbers around each atom in the configuration is generated using the utility **SCAT\_ABS.exe**. We recommend using  $R_{\text{max}} \leq 5 \text{ \AA}$  to ensure reasonable computation time.

This version of the RMCProfile software enables a simultaneous fit of electron (and/or X-ray single-crystal) diffuse scattering along with x-ray/neutron total scattering and EXAFS datasets. The importance of *single-crystal* diffuse scattering data, as obtained using electron diffraction, in local-structure refinements is evident from the results obtained by fitting the synthetic data simulated for a cubic perovskite KNbO<sub>3</sub> with correlated atomic displacements, which is presented in Appendix A4 of this manual. A number of electron diffraction patterns that can be included in the fit is limited only by the amount of the available computer RAM and reasonable computation times. Appendix A5 describes an effective and robust algorithm for subtraction of incoherent scattering. The algorithm is illustrated using the data for a metal hydride but is equally applicable to other systems including nanoparticles.

## 2. EXAFS

### 2.1 Technical background

#### 2.1.1 Single Scattering

Single scattering (two-leg path) contributions to EXAFS for the  $i^{\text{th}}$  absorber and  $j^{\text{th}}$  scatterer are calculated according to a formula given in the FEFF manual:

$$\chi_{ij}^{(1)} = \frac{S_i^2 \Re(k) |F_j(\pi, k)|}{kr_{ij}^2} \sin(2kr_{ij} + 2\delta_i(k) - l\pi + \varphi_j(\pi, k)) \exp(-2r_{ij}/\lambda(k)) \quad (1)$$

where  $S_i^2$  is the amplitude reduction factor,  $\Re(k)$  is the total central-atom loss factor,  $r_{ij}$  is the interatomic distance,  $k$  is the photoelectron wave number,  $F_j(\pi, k) = |F_j(\pi, k)| \exp(\varphi_j(\pi, k))$  is the complex backscattering amplitude,  $[2\delta_i(k) - l\pi]$  is the total scattering phase shift for the absorbing atom, and  $\lambda(k)$  is the photoelectron mean free path.

Functions  $S_i^2$ ,  $\Re(k)$ ,  $2\delta_i(k) - l\pi$ ,  $\lambda(k)$ ,  $|F_j(\pi, k)|$  and  $\varphi_j(\pi, k)$  are calculated by FEFF. A utility program **EXAFS\_INTER.exe** is used to interpolate these functions to  $k$ -mesh of the experimental data sets and store the parameters in the **\*.nsc1** file (see Section 5.1).

#### 2.1.2 Double and Triple Scattering

The exact equation for a double-scattering (i.e. a three-leg path, Fig. 1) contribution that involves an absorber  $i$  and scatterers  $j$  and  $n$  is expressed as:

$$\chi_{ijn}^{(2)} = \text{Im} C(\vartheta_{nij}) \frac{S_i^2 \Re F_j(\vartheta_{ijn}, k) F_n(\vartheta_{jni}, k)}{kr_{ij} r_{jn} r_{ni}} \exp(i(2kr_{\text{eff}} + 2\delta_i(k) - l\pi) - 2r_{\text{eff}}/\lambda(k)) \quad (2)$$

Here,  $r_{\text{eff}}=1/2(r_{ij}+r_{jn}+r_{ni})$  is the effective scattering-path length,  $F_j(\vartheta_{ijn}, k) = |F_j(\vartheta_{ijn}, k)| \exp(i\varphi_j(\vartheta_{ijn}, k))$  is the complex scattering amplitude for an atom  $j$  and the scattering angle  $\vartheta_{ijn}$ , and  $C(\vartheta_{nij})$  is the angle-dependent parameter (in the plane-wave approximation  $C(\vartheta_{nij}) = \cos(\vartheta_{nij})$ ).

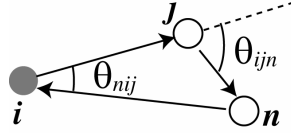


Fig. 1: A schematic representation of double scattering in a three-leg path. The scattering process involves an absorber  $i$  and scatterers  $j$  and  $n$ .

The FEFF code provides two real functions as an output:

$$F^{\text{effective}}(k) = \frac{|C(\vartheta_{nij})F_j(\vartheta_{ijn}, k)F_n(\vartheta_{jni}, k)|}{r_{ij}r_{jn}r_{ni}} r_{\text{eff}}^2$$

$$\varphi^{\text{effective}}(k) = \arg C(\vartheta_{nij})F_j(\vartheta_{ijn}, k)F_n(\vartheta_{jni}, k)$$

These functions can be substituted into Eq. (1) to calculate an EXAFS signal as implemented, for example, in the IFEFFIT/Artemis software. Similarly, in the present RMC calculations, the contribution of double scattering to EXAFS is calculated using the approximate formula:

$$\chi_{ijn}^{(2)} = \frac{S_i^2 \Re F_{jn}^{\text{eff}(2)}(\vartheta, k)}{kr_{ij}r_{jn}r_{ni}} \sin(2kr_{\text{eff}} + 2\delta_i(k) - l\pi + \varphi_{jn}^{\text{eff}(2)}(\vartheta, k)) \exp(-2r_{\text{eff}}/\lambda(k)), \quad (3)$$

where the effective amplitude factor is

$$F_{jn}^{\text{eff}(2)}(\vartheta, k) = \frac{|C(\vartheta_{nij})F_j(\vartheta_{ijn}, k)F_n(\vartheta_{jni}, k)|}{r_{0\text{eff}}^2} r_{0ij}r_{0jn}r_{0ni},$$

and the effective phase correction is

$$\varphi_{jn}^{\text{eff}(2)}(\vartheta, k) = \arg(C(\vartheta_{nij})F_j(\vartheta_{ijn}, k)F_n(\vartheta_{jni}, k)).$$

Here  $r_{0ij}$  is the distance between the atoms  $i$  and  $j$  in the cluster used in FEFF calculations.

Similarly, the contributions of the triple-scattering paths (Fig. 2) that involve either one or two scatterers are calculated according to the approximate formulae:

$$\chi_{ijn}^{(3)} = \frac{S_i^2 \Re F_{jn}^{\text{eff}(3)}(\vartheta_{ijn}, k)}{kr_{ij}^2 r_{jn}^2} \sin(2kr_{\text{eff}} + 2\delta_i(k) - l\pi + \varphi_{jn}^{\text{eff}(3)}(\vartheta_{ijn}, k)) \exp(-2r_{\text{eff}}/\lambda(k)) \quad (4a)$$

$r_{\text{eff}}=r_{ij}+r_{jn}$  (Fig. 2a)

$$\chi_{ij}^{(3)} = \frac{S_i^2 \Re F_j^{eff(3)}(\pi, k)}{kr_{ij}^4} \sin(2kr_{eff} + 2\delta_i(k) - l\pi + \varphi_j^{eff(3)}(\pi, k)) \exp(-2r_{eff}/\lambda(k)) \quad (4b)$$

$r_{eff}=2r_{ij}$ , (Fig. 2b)

$$\chi_{ijn}^{(3)} = \frac{S_i^2 \Re F_{jn}^{eff(3)}(\vartheta_{nij}, k)}{kr_{ij}^2 r_{in}^2} \sin(2kr_{eff} + 2\delta_i(k) - l\pi + \varphi_{jn}^{eff(3)}(\vartheta_{nij}, k)) \exp(-2r_{eff}/\lambda(k)) \quad (4c)$$

$r_{eff}=r_{ij}+r_{in}$  (Fig. 2c)

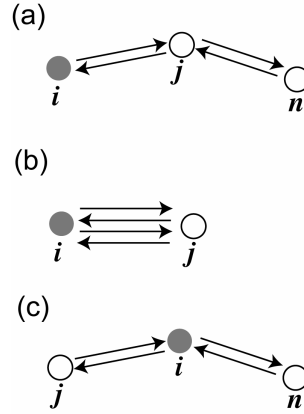


Fig. 2: Schematic representations of triple scattering paths that involve two scatterers (a, c) and a single scatterer (b).

Triple-scattering paths that involve three different scatterers are neglected in the present RMC refinements because of their small effect on the EXAFS signal.

Calculations of the effective amplitude factors and phase corrections are time consuming. Therefore, these characteristics are calculated prior to RMC refinements on the appropriate  $k$  and  $\vartheta$  meshes as described below in Sections 2.2, 2.3. During the refinements, the scattering amplitudes for the intermediate values of  $\vartheta$  are calculated using linear interpolation.

### 2.1.3 Double and Triple Scattering In the Nearly-Collinear Chains

Double- and triple-scattering paths that yield significant contributions to EXAFS involve nearly ( $\pm 30^\circ$ ) collinear chains (Figs. 1, 2) containing the intervening atom (i.e. atom  $j$  in Figs. 1, 2) in the first coordination shell of the absorber. In principle, scattering amplitudes and phase shifts depend on all three angles within the atomic triangle formed by the absorber and the scatterers. However, the present code assumes that for the nearly collinear chains these parameters are determined entirely by the  $\vartheta_{ijn}^{\lambda}$  angle; this simplifying, yet sufficiently accurate, assumption was introduced to speed up the calculations. A utility program **EXAFS\_INTER.exe** is used to calculate the amplitudes and phase shifts as a function of  $\vartheta_{ijn}^{\lambda}$  on a  $\vartheta$ -mesh selected by the user, and write the resulting data for all double and triple scattering paths into **\*.n<sub>1</sub>n<sub>2</sub>n<sub>3</sub>c2** and **\*.n<sub>1</sub>n<sub>2</sub>n<sub>3</sub>c3** files respectively, as detailed in Section 5.2.,

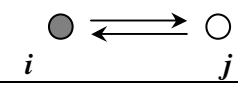

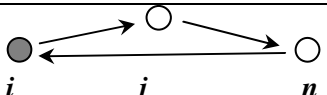

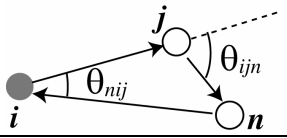
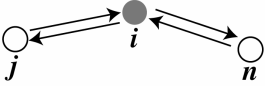
### 2.1.4 Double and Triple Scattering In the Nearest Coordination Spheres

Another important geometry for double scattering involves triangular paths with the scatterers located in the 1<sup>st</sup> and 2<sup>nd</sup> coordinations shells around the absorber (Figs. 1b). In this case, the effective amplitude factors and phase corrections are determined primarily by the  $\vartheta_{nij}$  angles. Again, a utility program **EXAFS\_INTER.exe** is used to calculate the amplitudes and phase shifts as a function of  $\vartheta_{nij}$  on the  $\vartheta$ -mesh selected by the user (Section 5.3) and store the resulting data for this type of double-scattering paths in the file **\*.n<sub>1</sub>n<sub>2</sub>n<sub>3</sub>s2**.

The amplitude and phase parameters for the triple-scattering paths shown in Figs. 2b are stored in the file **\*.nsc3**. Similar tables for the triple-scattering paths shown in the Fig. 2c are stored in the file **\*.n<sub>1</sub>n<sub>2</sub>n<sub>3</sub>s2**.

## 2.2 The EXAFS files for combined PDF/EXAFS refinements

Below is a list of files required to run RMCProfile with EXAFS data included in the refinements:

Filename	Path pictogram	File Content
<b>*.n<sub>1</sub>sc1</b>		photoelectron mean free path; moduli and phases of backscattering amplitudes for the single-scattering paths;
<b>*.n<sub>1</sub>sc3</b>		amplitude factors and phase corrections for the triple-scattering paths
<b>*.n<sub>1</sub>n<sub>2</sub>n<sub>3</sub>c2</b>		effective amplitude factors and phase corrections for the double-scattering paths in nearly collinear atomic chains
<b>*.n<sub>1</sub>n<sub>2</sub>n<sub>3</sub>c3</b>		effective amplitude factors and phase corrections for the triple-scattering paths in nearly collinear atomic chains
<b>*.n<sub>1</sub>n<sub>2</sub>n<sub>3</sub>s2</b>		effective amplitude factors and phase corrections for the double-scattering paths having both scattering atoms in the 1 <sup>st</sup> and 2 <sup>nd</sup> coordination shells around the absorber
<b>*.n<sub>1</sub>n<sub>2</sub>n<sub>3</sub>s3</b>		effective amplitude factors and phase corrections for the triple-scattering paths with the two scattering atoms located in the 1 <sup>st</sup> coordination shell around the absorber, and the absorber atom itself acting as a scatterer
<b>absorlist.dat</b>		list of absorber atoms around each atom in the configuration
<b>scattlist.dat</b>		list of all scattering atoms for each absorber

In the filenames,  $n_1$  stands for the type of the absorbing atom,  $n_2$  for the type of the distant scatterer, and  $n_3$  for the type of the intervening scatterer in  $*.n_1n_2n_3c2(3)$  files; in the files  $*.n_1n_2n_3s2(3)$ ,  $n_2$  and  $n_3$  represent types of the scattering atoms.

## 2.3 Preparation of the EXAFS Data.

Preliminary analyses of EXAFS data are needed to obtain accurate values of the energy shifts,  $E_0$ , and to subtract the background from the data, as following:

- (a) Use Athena (or similar) to extract EXAFS from the absorption spectra.
- (b) For each experimental EXAFS build an appropriate cluster(s) around the absorbing atom. An average structure provides a good starting model. Examples of public domain software that can be used to generate these clusters based on the space group and atomic positions include Atoms/Artemis. For structures with the same absorber species located in non-equivalent crystallographic positions, separate clusters have to be generated for each of these sites. These non-equivalent sites must be designated using distinct atom types in the \*.cfg file. The contributions of these clusters to the total EXAFS signal are set proportional to the respective site occupancies.
- (c) Perform self-consistent FEFF calculations of the scattering paths in a separate folder for each cluster. In the FEFF input file, set the amplitude-reduction parameter  $S_0^2$  to a value less than 0.1 to let FEFF estimate this parameter from the atomic overlap integrals. Identify scattering paths to be used in the fit.
- (d) Use Artemis (or similar) to fit the experimental EXAFS using selected scattering paths. For all paths, set  $S_0^2$  ('amp' parameter in the GDS section) to a value calculated by FEFF. (FEFF8.20 provides satisfactorily estimates for  $S_0^2$ ), which are specified in the header of the **chi.dat** output file. The fitted value of  $S_0^2$  may deviate from the theoretical due, for example, to inhomogeneous sample; significant deviations likely indicate a problem and should be considered seriously. If multiple experimental EXAFS datasets are available, a simultaneous fit is recommended. Each dataset should be assigned a single value of  $E_0$ .
- (e) Return to the EXAFS data-reduction software (e.g. Athena) and adjust  $E_0$  to the fitted value to convert EXAFS oscillations from the energy- to  $k$ -space. Repeat the fit in Artemis using these modified data and obtain a new value of  $E_0$ . Repeat this procedure iteratively until  $E_0 < 0.5$  eV. This process minimizes systematic errors caused by the incorrect choice of  $E_0$ .
- (f) In Artemis, fit the background, if possible, and save the experimental data and the background as chi(k).
- (g) Use any spreadsheet software (e.g. Excel) to subtract the background from the experimental data. The background subtraction option in the current version of Artemis appears to work incorrectly.
- (h) Save the background-subtracted experimental data in the following format:  
1<sup>st</sup> line – number of experimental points;  
2<sup>nd</sup> line – title;  
Subsequent lines –  $k$  ( $\text{\AA}^{-1}$ ) and  $\text{chi}(k)$  values in  $xy$  format.

## 2.4 Creating EXAFS files

In the following, the file structures are illustrated using perovskite-like  $\text{SrAl}_{1/2}\text{Nb}_{1/2}\text{O}_3$  as an example. EXAFS data for Sr and Nb are stored in the files I\_Sr-back.dat and I\_Nb-back.dat respectively. In the \*.cfg file, the atom types are specified as 1-Sr, 2-Nb, 3-Al, 4-O.

Create a separate folder for each absorber type and perform FEFF calculations for all the absorbers.

- (a) Each of these folders should contain the following files/subfolders: (1) EXAFS\_INTER.exe file, (2) FEFFxxx.exe file, (3) experimental EXAFS datafile, (4) **feff.inp** file generated by Artemis, (5) **path.dat** file generated by FEFF, and (6) a subfolder called “store” where the output files will be stored;
- (b) Rename the **path.dat** file created by FEFF to **pathbackup.dat**. An example of the **path.dat** file and the description of its structure are presented in Appendix A1;
- (c) Open **feff.inp** file and change the CONTROL card parameters to  
CONTROL 0 0 0 0 1 1 for FEFF820.exe or to  
CONTROL 0 0 1 1 for FEFF61.exe
- (d) Identify the paths to be included in the fit;
- (e) Run EXAFS\_INTER.exe. Respond to the prompts. The “reduction factor” is the  $S_0^2$  parameter obtained in the preliminary fit.

The following menu will appear:

```

C:\Documents and Settings\Krazzman\My Documents\Visual Studio 2005\Projects\Console8...
Enter 1 for single scattering
Abs->Scat->Abs

Enter 2 for triple scattering from the same scatterer
Abs->Scat"1"->Abs->Scat"1"->Abs

Enter 3 for chain-like scattering
Abs->Interv_Scat->Distant_Scat->Abs and
Abs->Interv_Scat->Distant_Scat->Interv_Scat->Abs

Enter 4 for non-chain double scattering
Abs->Scat"1"->Scat"2"->Abs

Enter 5 for triple scattering from different scatterers
Abs->Scat"1"->Abs->Scat"2"->Abs

Enter 0 to exit
  
```

Select the appropriate option(s) and enter the following information:

### Option 1

Enter a sequence of file numbers xxxx for the feffxxxx.dat files corresponding to all single-scattering paths. An output file **\*.n1sc1** will be generated.

### Option 2

Enter a sequence of file numbers xxxx for the feffxxxx.dat files corresponding to all triple-scattering paths, which involve one scattering (not absorbing) atoms and the absorbing atom as the second scatterer. An output file **\*.n<sub>1</sub>sc3** will be generated.

### Option 3

Enter the types of the distant and intervening scatterers for a double-scattering *chain-like* process and the number xxxx of the feffxxxx.dat file corresponding to this forward-scattering path. A value of the scattering angle for the selected path will be displayed. Enter the minimum and maximum values (in degrees) for the angular range to be sampled. An output file **\*.n<sub>1</sub>n<sub>2</sub>n<sub>3</sub>c2** will be generated. Enter the number xxxx of the feffxxxx.dat file corresponding to the triple-scattering path. An output file **\*.n<sub>1</sub>n<sub>2</sub>n<sub>3</sub>c3** will be generated. In order to include similar scattering processes for another set of the distant and intervening scatterers, select option 3 again and follow the same procedure.

### Option 4

Enter the types of scatterers for a double-scattering *not chain-like* process. Several nonequivalent paths may exist that include the same types of scatterers. Enter the total number of these paths and, then, the numbers xxxx of the corresponding feffxxxx.dat files in the ascending order for the internal angle (angle  $\theta_{nij}$  for a triangular path is defined in Fig. 1). As the number of the feffxxxx.dat file corresponding to the the smallest angle is entered, a value of this angle will be displayed. Enter the minimum and the maximum values (in degrees) for the angular range to be sampled. The procedure will be repeated for every double-scattering path with the specified scatterers. The angle intervals selected for different non-equivalent paths involving the same scatterers should not overlap. In order to specify the double-scattering processes for other types of scatterers select option 4 again.

### Option 5

Enter the types of scatterers for a triple-scattering *not chain-like* process. Several nonequivalent paths may exist that include the same types of scatterers. Enter the total number of these paths and, then, the numbers xxxx of the corresponding feffxxxx.dat files in the ascending order of the internal angle (angle  $\theta_{nij}$  for a triangular path is defined in Fig. 1). As the number of the feffxxxx.dat file corresponding to the the smallest angle is entered, a value of this angle will be displayed. Enter the minimum and the maximum values (in degrees) for the angular range to be sampled.. The procedure will be repeated for every triple scattering path with the specified scatterers. The angle intervals selected for different non-equivalent paths involving the same scatterers should not overlap. In order to specify the double-scattering processes for other types of scatterers select option 5 again.

## 2.5 Creating lists of absorbing and scattering atoms

These lists are generated using the utility **SCAT\_ABS.exe** and stored in the files **absorlist.dat** (Appendix A2) and **scattlist.dat** (Appendix A3). For running **SCAT\_ABS.exe**, copy the initial configuration file **\*.cfg** into a folder which contains **SCAT\_ABS.exe**. In the same folder, create an input file **scat\_input.txt**. An example of the input file is shown below:



```

SrAlNbO3.cfg
2                                ! NEXAFS - number of experimental spectra
1                                ! NABS - number of types of absorbers for a given spectrum
2  4.2 0.0  4.2 0.0  4.2 5.0  4.2 0.0
1
1  4.2 0.0  4.0 0.0  4.2 0.0  4.2 0.0

```

The first line is a name of the configuration file. The second line is a number of the experimental EXAFS datasets (NEXAFS). This line is followed by NEXAFS groups of lines. The total number of these groups and their order must correspond to the order of the EXAFS groups in the RMCProfile \*.dat file.

The first line of each group specifies the number of types of absorbers for a given EXAFS dataset (NABS). This line is followed by one line per absorber. In this line, the first digit specifies the type of the corresponding absorbing atom. This digit is followed by *ntypes* pairs of real numbers, where *ntypes* is the number of types of atoms in the configuration file. The first number in the pair is the maximum distance between the corresponding scattering atoms and the absorbing atoms to be included the list. The second number is the maximum scattering angle to search for an intervening atom for the chain scattering that involves these absorbing and scattering types.

### 3. Diffuse scattering in Electron Diffraction

#### 3.1. Diffuse scattering calculations

The calculations of diffuse scattering were implemented according to the formalism proposed by Butler and Welberry (*B. D. Butler, T. R. Welberry, J. Appl. Cryst.* 25, 391, 1992) and later adopted for RMC refinements using electron diffraction by Goodwin *et al.* (*A. L. Goodwin, R. L. Withers, H. B. Nguyen, J. Phys. Cond. Matter*, 19(33), 335216, 2007). According to this formalism, the complex total scattering amplitude  $A_{\text{tot}}(\mathbf{k})$  is calculated in the kinematic approach as

$$A_{\text{tot}}(\mathbf{k}) = \sum_{\mathbf{n}} \sum_{m=1}^M f_m(k) \exp(i\mathbf{k}(\mathbf{R}_{\mathbf{n}} + \mathbf{r}_{m\mathbf{n}})), \quad (6)$$

where  $\mathbf{k}=(k_x, k_y, k_z)$  is the diffraction vector,  $\mathbf{R}_{\mathbf{n}}=(a n_x, b n_y, c n_z)$  is a vector that describes the origin of the  $\mathbf{n}^{\text{th}}$  unit cell,  $\mathbf{r}_{m\mathbf{n}}=(x_{m\mathbf{n}}, y_{m\mathbf{n}}, z_{m\mathbf{n}})$  is a vector that describes the position of the  $m^{\text{th}}$  atom in the  $\mathbf{n}^{\text{th}}$  cell,  $f_m(k)$  is the atomic scattering factor,  $a$ ,  $b$ , and  $c$  are the lattice parameters,  $N_x$ ,  $N_y$ , and  $N_z$  specify the number of unit cells along the corresponding axes of the the configuration box,  $N=N_x N_y N_z$  is the total number of the unit cells in the box, and  $M$  is the number of atoms in the unit cell,  $0 \leq n_{\alpha} \leq N_{\alpha}-1$  ( $\alpha \in [x, y, z]$ )

The average scattering amplitude  $\langle A(\mathbf{k}) \rangle$  is calculated as

$$\langle A(\mathbf{k}) \rangle = \frac{1}{N} \sum_{\mathbf{n}} \sum_{m=1}^M f_m(k) \exp(i\mathbf{k}(\mathbf{r}_{m\mathbf{n}})). \quad (7)$$

The amplitude of diffuse scattering  $A_D(\mathbf{k})$  is a difference

$$A_D(\mathbf{k}) = A_{tot}(\mathbf{k}) - \langle A(\mathbf{k}) \rangle \psi(\mathbf{k}), \quad (8)$$

where the interference function  $\psi(\mathbf{k})$  is

$$\psi(\mathbf{k}) = \sum_{\mathbf{n}} \exp(i\mathbf{k}\mathbf{R}_{\mathbf{n}}) = \frac{\exp(ik_x a N_x) - 1}{\exp(ik_x a) - 1} \cdot \frac{\exp(ik_y b N_y) - 1}{\exp(ik_y b) - 1} \cdot \frac{\exp(ik_z c N_z) - 1}{\exp(ik_z c) - 1}. \quad (9)$$

The intensities in experimental electron diffraction patterns are affected by multiple scattering and therefore cannot be reproduced by calculations that rely on the kinematic approximation. Therefore, only the locus of diffuse scattering, which reflects the topology of correlations in real space, is fitted; the information on the magnitude of correlation parameters can be recovered only to the extent that is encoded in the total scattering and EXAFS data. In the present fitting procedure, the experimental (relative units) and calculated intensities are matched using the scale factor and the offset which are adjusted after each RMC move. As an option, the scale and offset factors can be kept fixed. Both logarithmic (appropriate for film recording)  $I_D(\mathbf{k}) = \ln|A_D(\mathbf{k})|^2$  and linear (digital detectors)  $I_D(\mathbf{k}) = |A_D(\mathbf{k})|^2$  intensity scales are implemented. .

Experimental diffraction patterns are assumed to be centered on the reciprocal space origin and exhibit a two-fold rotation symmetry axis. For diffraction patterns exhibiting mirror symmetry across two orthogonal planes, a single quadrant is used as an input and the second adjacent quadrant is generated automatically by the software according to the mirror symmetry; the resulting half plane is used in the fit. For diffraction patterns without mirror symmetry, a half plane is used as an input. The input files are generated using the **ED.exe** utility program.

### 3.2. Noise reducing and background subtracting

Typically, the total scattering amplitude calculated for a single atomic configuration by direct summation (6) is too noisy to be effectively used in the fit. In the present software, the noise is reduced using two complementary procedures. First, the use is made of the periodic boundary conditions imposed in the RMC refinements. The position of an atom in the configuration is described by a sum  $\mathbf{R}_{\mathbf{n}} + \mathbf{r}_{mn}$ . Therefore, the transformation of the atomic coordinates according to the formulae

$$\begin{aligned} an_x + x_{mn} &\rightarrow \begin{cases} a(n_x - l_x) + x_{mn} & \text{for } l_x \leq n_x < N_x \\ a(n_x - l_x + N_x) + x_{mn} & \text{for } 0 \leq n_x < l_x \end{cases} \\ bn_y + y_{mn} &\rightarrow \begin{cases} b(n_y - l_y) + y_{mn} & \text{for } l_y \leq n_y < N_y \\ b(n_y - l_y + N_y) + y_{mn} & \text{for } 0 \leq n_y < l_y \end{cases}, \\ cn_z + z_{mn} &\rightarrow \begin{cases} c(n_z - l_z) + z_{mn} & \text{for } l_z \leq n_z < N_z \\ c(n_z - l_z + N_z) + z_{mn} & \text{for } 0 \leq n_z < l_z \end{cases} \end{aligned} \quad (10)$$

generates the atomic configuration equivalent to the original. The total scattering amplitude calculated for the new configuration using Equation (6) is somewhat different compared to that calculated for the original configuration, whereas the average scattering amplitude remains unchanged. According to the present procedure, the  $I_D(\mathbf{k})$  calculated after each RMC move is averaged over eight equivalent configurations with  $l_x=0, [N_x/2]$ ;  $l_y=0, [N_y/2]$ ;  $l_z=0, [N_z/2]$ . The maximum number of equivalent configurations that could be included in the averaging is  $N$ , but using so many configurations would make the computations prohibitively expensive.

The noise is further reduced by binning of the diffuse scattering intensity image according to

$$\langle I_D(i, j) \rangle = \{I_D(i, j) + 0.5[I_D(i+1, j) + I_D(i, j+1) + I_D(i-1, j) + I_D(i, j-1)] + 0.25[I_D(i+1, j+1) + I_D(i-1, j+1) + I_D(i-1, j-1) + I_D(i+1, j-1)]\} / 4, \quad (11)$$

where  $i$  and  $j$  refer to the pixel numbers.

A continuous part of diffuse scattering caused, for example, by displacive (thermal) disorder, correlated displacements, etc, acts as a background for the structured diffuse scattering and effectively reduced the contrast especially on the logarithmic scale. Therefore, this background is removed prior to the fit. The background  $B(k)$  is considered to be isotropic with its  $\mathbf{k}$ -vector dependence determined primarily by the rapid decay of atomic scattering factors with increasing  $\mathbf{k}$ . The dependence  $B(k)$  is fitted using an analytical expression

$$B(k) = P_1 \exp(-P_2 k^2) + P_3, \quad (12)$$

where  $P_i$  are adjustable parameters, and subtracted from the calculated diffuse scattering.

### 3.3. Atomic scattering factor calculations

The atomic scattering factors for electron diffraction are calculated using the traditional parameterization according to the formula (Peng L-M, *Acta Cryst.*, A54, 481, 1998)

$$f_m(k) = \sum_{j=1}^5 a_j \exp(-b_j k^2) + \frac{me^2}{8\pi^2 \hbar^2 k^2} \Delta Z, \quad (11)$$

where  $a_j$  and  $b_j$  are tabulated parameters (Peng L-M, *Acta Cryst.*, A54, 481, 1998),  $\Delta Z$  represents the ionic charge, the pre-factor  $\frac{me^2}{8\pi^2 \hbar^2} = 0.023934$  if  $k$  is given in  $\text{\AA}^{-1}$  and  $f_m(k)$  is in  $\text{\AA}$ . The values of  $a_j$  and  $b_j$  are stored in the file **FormfactorsTable.dat**. The **FormfactorsTable.dat** consists of three-line blocks for each type of atoms in the configuration. The first line in a block is a chemical symbol for a given atom type, the second line contains five real values of  $a_j$ , and the third line contains five real values of  $b_j$ .

The order of blocks in the file is not important. A user can modify this file using any text editor. Ionic charges (valences) should be specified as real numbers in the \*.dat file after the keyword "VALENCE ::". The valences must be listed in the same order as the atoms in the "ATOMS ::" line.

### 3.4. Input and output files

The input files, each containing a distribution of diffuse intensity in a given section of reciprocal space to be included in the fit, are produced using the **ED.exe** utility program from the digitized experimental electron diffraction patterns. The procedure for generating these input files is detailed in Section 3.5. The first line of the input file is an integer which specifies a number of the data lines in the file. The second line is a logical constant which is set to **.true.** for diffraction patterns having mirror symmetry and to **.false.** otherwise. For patterns without mirror symmetry, each subsequent line contains two integer numbers representing pixel coordinates and three real numbers describing the reciprocal-space coordinates ( $x, y$ ) of this point in  $\text{\AA}^{-1}$  and the corresponding intensity value. For those patterns that exhibit mirror symmetry, each line additionally includes three coordinates of the point related by mirror symmetry to the corresponding point in the chosen quadrant.

Three kinds of output files are produced for each diffraction pattern used in the fit. The graphic files **exper\_diffuse\_n.bmp** and **calcul\_diffuse\_n.bmp** (**calcul\_diffuseS\_n.bmp**) facilitate visual comparison of the experimental and calculated patterns for the  $n^{\text{th}}$  dataset. A digital output is provided in the files **diffuse\_intensity\_outn.dat** (**diffuse\_intensity\_outSn.dat**) which are saved after a user-specified run time along with other output files (e.g. total scattering and/or EXAFS). The first three lines in this file contain values of the residual, a scale factor, and an offset for a given dataset. These lines are followed by a matrix describing the intensity distribution. Files **calcul\_diffuseS\_n.bmp** and **diffuse\_intensity\_outSn.dat** are produced only if the pattern exhibits mirror symmetry and contain intensities calculated for the symmetry related quadrants of reciprocal space. A file **backgroundn.dat** contains  $B(k)$  along with its fitted analytical representation. Calculated arrays of total  $A_{\text{tot}}(\mathbf{k})$  and average  $\langle A(\mathbf{k}) \rangle$  scattering amplitudes are saved simultaneously with other output files in the binary files **ScatAmpl.bin** (**ScatAmplS.bin**).

### 3.5. Input file processing

Commonly, experimental diffraction patterns containing diffuse scattering are recorded on a film. In this case, the experimental pattern has to be digitized using a suitable scanner or a similar device and stored in the .bmp format. The processing of the resulting image to produce an input data file for RMCProfile involves the following steps:

- a) Define the origin of the co-ordinate system for the image and determine its coordinates;
- b) Define two reciprocal space vectors in the image;
- c) Mask all the Bragg peaks which will be excluded from the fit;
- d) Choose an appropriate quarter of the diffraction pattern to be used in the fit.

The central spot in experimental electron diffraction patterns is saturated and, as such, is not suitable for precise determination of the origin. Instead, the center is found from the coordinates of several Bragg peaks located symmetrically around the central spot. The program **ED.exe** prompts the user to select suitable Bragg spots using mouse clicks. The program fits each of these peaks with a 2-D Gaussian (saturated portions of the peaks, if encountered, are excluded by the program) to find the peak positions. The position of the origin is calculated as an average of the Bragg peak positions.

The two reciprocal space vectors are defined (following the on-screen prompts) by using mouse clicks to select several orders for the two independent reflection families (e.g. 111, 222, 333 and 100, 200, 300) and specifying the *hkl* indexes for each of these peaks. The program automatically determines the precise positions of the selected peaks and the length of the corresponding reciprocal space vectors in  $\text{\AA}^{-1}$ .

The RMCProfile code fits only the diffuse component of electron scattering and, therefore, Bragg peaks must be excluded from the fitted pattern. This is accomplished by using masks which are placed on top of all the Bragg spots in the pattern. The mask has an ellipsoidal shape inscribed into a rectangular. The user selects the size of the mask by defining the upper left and lower right corners of this rectangular using mouse clicks as prompted by the program. Once the user selects one Bragg peak, the program automatically locates and masks its pair related by the  $180^\circ$  rotation around the centre.

Finally, the user selects the quarter of the diffraction pattern to be included in the fit (only one quarter is fitted to reduce the computation time) using a mouse click in the corresponding corner of the diffraction pattern. Once this action is completed, the program **ED.exe** creates an input file for use by RMCProfile. The name of this file must be specified in the `DIFFUSE_SCATTERING :: card` of the **\*.dat** file.

#### 4. Restraints on peak tails in partial PDFs

“DISTANCE WINDOW” and “MINIMUM DISTANCES” constraints frequently cause unphysical spikes/discontinuities in partial PDFs at the distance limits set by these constraints; usually, these limits and the spikes occurs in the tail portions of the PDF peaks. This effect is most pronounced in the case of two closely overlapped partial PDFs that exhibit opposite signs of the Faber-Ziman coefficients. In this case, the artificial spikes in the two PDFs cancel each other so that the total PDF exhibits no discontinuities; therefore, no driving force for “healing” these spikes exist during fitting of the total PDF. The problem can be alleviated by imposing restraints on the peak tails in partial PDFs as implemented in the current version of RMCProfile. These restraints can be applied to the low-*r* and/or high-*r* tails of any peak in any partial PDF. For each restraint, a user has to specify the  $r_{\min}$  (left) and  $r_{\max}$  (right) limits of the interval over which the constraint is applied along with the tail function  $L(r)$ . This function is defined as a fourth-order polynomial with a zero constant term:

$$L(r) = \sum_{n=1}^4 a_n (r - r_0)^n \quad (5)$$

where  $r_0$  is set to  $r_{\min}$  and  $r_{\max}$  for the low- $r$  tail and high- $r$  tails, respectively. The coefficients  $a_n$  must be obtained by fitting  $L(r)$  to the tail of interest using any suitable computer software. For a given partial PDF  $g_m(r)$ , the program checks the inequality  $g(r_j) > L(r_j)$  for all  $r_j \in [r_{\min}, r_{\max}]$  after each RMC move. If the condition is satisfied, the penalty function having a user-specified weight is added to the residual.

The restraint for each low- $r$  tail to be constrained is activated by including the following block of keywords in the **\*.dat** file:

```
LEFT_TAILS ::
> START_FINISH :: here,  $r_{\min}$  and  $r_{\max}$  for this tail must be specified
> PARTIAL :: integer corresponding to the number of a partial must be specified
> COEFFICIENTS :: 4 real numbers describing coefficients  $a_1$ ,  $a_2$ ,  $a_3$ , and  $a_4$ 
> WEIGHT :: weight assigned to the penalty function
```

The restraint for each high- $r$  tail to be constrained is activated using similar keywords with the major keyword RIGHT\_TAILS ::.

## 5. Major keywords in the \*.dat file

EXAFS ::	Introduces a block of data concerning a set of EXAFS data. Text can follow the :: but will be ignored. This keyword must be followed by a block of subordinate keywords. Each EXAFS spectrum requires a separate keyword and a block of data. <i>Do not include if no EXAFS data is fitted.</i>
LEFT_TAILS :: / RIGHT_TAILS ::	Introduces a block of data concerning restraints on the tails of peaks in partial PDFs. This keyword must be followed by a block of subordinate keywords. <i>Do not include if no restraints are used.</i>
DIFFUSE_SCATTERING ::	Introduces a block of data concerning electron diffraction pattern. Text can follow the :: but will be ignored. This keyword must be followed by a block of subordinate keywords. Each diffraction pattern requires a separate keyword and a block of data. <i>Do not include if no electron diffraction data is fitted.</i>
BOX_SIZES ::	Specifies the numbers of unit cells in the atomic box. Mandatory if DIFFUSE_SCATTERING is present.
VALENCE ::	Specifies the valence (charge) of ions for the atomic scattering factors calculations for diffuse scattering. The order of atoms must correspond to that in ATOMS keyword. Mandatory if DIFFUSE_SCATTERING is present.

## 6. Subordinate keywords in the \*.dat file

EXAFS ::

> FILENAME ::	Filename containing the data
>FIT_SPACE ::	Acceptable values: $r$ , $k$ ( <i>case-insensitive</i> ). Specifies whether a real (coordinate) space or a wave-vector space ( $k$ ) is used for the EXAFS fit.
> START_POINT_(R_SPACE) ::	Start point for a fit in the $r$ space (Å)
> END_POINT_(R_SPACE) ::	End point for a fit in the $r$ space (Å)
> R_SPACING ::	Value of the spacing used in the EXAFS fit and the output (Å).
> LOW_R_REGION_LIMIT::	(Optional) If specified, assigns additional factor to the lower- $r$ part contribution to the total misfit. This factor must be provided with the subordinate keyword >LOW_R_WEIGHT
> LOW_R_WEIGHT ::	An additional factor for the lower- $r$ part contribution to the total misfit in the case of $r$ -space fit
> START_POINT_(K_SPACE) ::	Start point of the fit in $k$ -space (if selected in >FIT_SPACE) or a Fourier transform for a fit in the $r$ space (Å <sup>-1</sup> )
> END_POINT_(K_SPACE) ::	End point of the fit in $k$ space or a Fourier transform for a fit in the $r$ space (Å <sup>-1</sup> )
> K_POWER ::	Specifies the power of $n$ in the weight-factor $k^n$ used to multiply EXAFS signal $\chi(k)$ prior to a Fourier transform
> WEIGHT ::	Parameter to weight the total misfit for the EXAFS data in Monte Carlo simulation
> ENERGY_OFFSET ::	(Optional) Shift of $E_0$ (eV) in the experimental spectrum. If not included, $E_0=0$
> SCALE_FACTOR ::	(Optional) Scale factor for the experimental spectrum (optional). If not included, scale factor=1
> NUMBER_OF_TYPES_OF_ABSORBING_ATOMS::	(Optional) Specifies the number of types of absorbing atoms for a given EXAFS dataset. If not included, the number of types is set to 1.
> TYPE(S)_OF_ABSORBING_ATOMS::	A list of types of the absorbing atoms for a given EXAFS dataset

LEFT\_TAILS :: (RIGHT\_TAILS ::)

> START_FINISH ::	$r_{\min}$ and $r_{\max}$ values (Å)
> PARTIAL ::	Number of partials to which the restraint is applied

> COEFFICIENTS ::	Coefficients $a_1$ , $a_2$ , $a_3$ , and $a_4$ in Equation (5)
> WEIGHT ::	Weight of the penalty function due to the tail restraint

DIFFUSE\_SCATTERING ::

> FILENAME ::	Filename containing the data
> WEIGHT ::	Parameter to weight the total misfit for the diffuse scattering data in Monte Carlo simulation.
> CONSTANT_OFFSET :: or > FITTED_OFFSET ::	Indicates whether constant or fitted offset is used for calculated diffuse scattering. In the case of constant offset its value must be supplied after ::
> CONSTANT_SCALE :: or > FITTED_SCALE ::	Indicates whether constant or fitted scale is used for calculated diffuse scattering. In the case of constant scale its value must be supplied after ::
> LINEAR :: or > LOGARITHMIC ::	Specifies the type of intensity scale for diffuse scattering. Mandatory if DIFFUSE_SCATTERING is present.



## Appendix

### A1. The Pathsbackup.dat file

```
...  
Rmax 6.0000, keep limit 0.000, heap limit 0.000 Feff 6L.02 paths 3.05  
Plane wave chi amplitude filter 2.50%
```

```
-----  
  1  2  6.000  index, nleg, degeneracy, r= 1.9805  
    x      y      z  ipot  label  rleg  beta  eta  
0.000000  0.000000  1.980540  4  'O  '  1.9805  180.0000  0.0000  
0.000000  0.000000  0.000000  0  'Nb '  1.9805  180.0000  0.0000  
  
  2  2  8.000  index, nleg, degeneracy, r= 3.3764  
    x      y      z  ipot  label  rleg  beta  eta  
-1.949350  1.949350 -1.949350  1  'Sr '  3.3764  180.0000  0.0000  
0.000000  0.000000  0.000000  0  'Nb '  3.3764  180.0000  0.0000  
  
  3  3  24.000  index, nleg, degeneracy, r= 3.3810  
    x      y      z  ipot  label  rleg  beta  eta  
1.980540  0.000000  0.000000  4  'O  '  1.9805  135.0000  0.0000  
0.000000 -1.980540  0.000000  4  'O  '  2.8009  135.0000  0.0000  
0.000000  0.000000  0.000000  0  'Nb '  1.9805   90.0000  0.0000  
  
  4  2  6.000  index, nleg, degeneracy, r= 3.8987  
    x      y      z  ipot  label  rleg  beta  eta  
0.000000 -3.898700  0.000000  3  'Al '  3.8987  180.0000  0.0000  
0.000000  0.000000  0.000000  0  'Nb '  3.8987  180.0000  0.0000  
  
  5  3  12.000  index, nleg, degeneracy, r= 3.8987  
    x      y      z  ipot  label  rleg  beta  eta  
0.000000  0.000000 -3.898700  3  'Al '  3.8987  180.0000  0.0000  
0.000000  0.000000 -1.980540  4  'O  '  1.9182   0.0000  0.0000  
0.000000  0.000000  0.000000  0  'Nb '  1.9805  180.0000  0.0000  
  
  6  4  6.000  index, nleg, degeneracy, r= 3.8987  
    x      y      z  ipot  label  rleg  beta  eta  
-1.980540  0.000000  0.000000  4  'O  '  1.9805   0.0000  0.0000  
-3.898700  0.000000  0.000000  3  'Al '  1.9182  180.0000  0.0000  
-1.980540  0.000000  0.000000  4  'O  '  1.9182   0.0000  0.0000  
0.000000  0.000000  0.000000  0  'Nb '  1.9805  180.0000  0.0000
```

### A2. The absorlist.dat file

```
20480  total number of lines equal to the total number of atoms in cfg  
14      maximal number of absorbers in a line  
10 4097 2  4609 2  5121 2  5633 2  2049 1  2056 1  2561 1  2617 1  3073 1  
3521 1  
10 4098 2  4610 2  5122 2  5634 2  2049 1  2050 1  2562 1  2618 1  3074 1  
3522 1  
  
8  194 1  706 1  1218 1  1730 1  2242 1  2754 1  3266 1  3778 1  
  
14 4609 2  5057 2  ...      ...  576 1  1480 1  2041 1  2056 1  2617 1  3521 1  
4096 1
```

### A3: The scattlist.dat file

```
6144 total number of lines
26 maximal number of scatterers in a line
26 2049 1 0 0 ... 3073 1 0 0

20 181 1 0 0 .....6901 3 10933 4 7349 3 13493 ..... 20149 4 0 0
```

### A4. Example of a combined fit of neutron total PDF, Bragg profile, and electron diffuse scattering

The cubic phase of perovskite-like  $\text{KNbO}_3$  is believed to exhibit 8-site displacive disorder associated with random local displacements of Nb along 8 non-equivalent  $\langle 111 \rangle$  directions. The displacements are correlated along the -Nb-O-Nb- linear chains parallel to  $\langle 100 \rangle$  directions. Similar 8-site disorder is encountered in perovskite  $\text{BaTiO}_3$  and  $\text{AgNbO}_3$  as well as their solid solutions with other perovskite compounds. The correlated displacements are manifested in three orthogonal sets of  $\{100\}$  sheets of diffuse intensity passing through all fundamental reflections; the diffuse intensity is extinct through the origin of reciprocal space because the correlated displacement components are directed parallel to the correlation directions. In the present example we used synthetic data simulated for a large atomic configuration that mimicked the 8-site disorder for Nb to determine whether the correct displacement correlations can be recovered at least using error-free data. The simulated data that was used in these analyses included neutron PDF and electron diffuse scattering.

The structure model used to simulate the data was based on the configuration cell of  $64 \text{ \AA} \times 64 \text{ \AA} \times 64 \text{ \AA}$ , which contained 20,480 atoms located at the ideal lattice sites of the cubic perovskite structure. The Nb atoms were shifted along  $\langle 111 \rangle$  directions  $0.1\sqrt{3} \text{ \AA}$  and the O atoms were shifted along  $\langle 001 \rangle$  direction by  $0.1 \text{ \AA}$  to generate positive Nb-Nb and negative Nb-O displacement correlations along the  $\langle 001 \rangle$  -Nb-O-Nb-  $\langle 001 \rangle$  chains; the displacements among different chains remained uncorrelated thus yielding the desired 8-site model (Figure A4.1). Subsequently, all atoms in the configuration were subjected to random Gaussian displacements. The total neutron pair-distribution function (PDF) and Bragg profile were calculated for this model configuration and used instead of experimental datasets in the RMC fits.

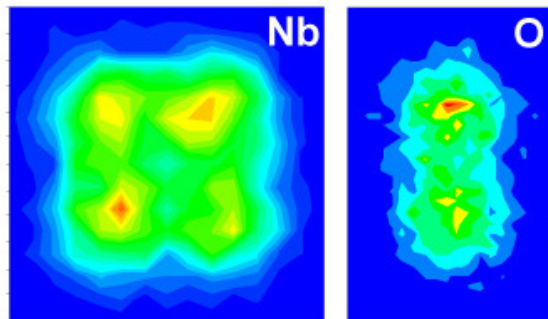


Figure A4.1: Probability density distribution functions for Nb and O viewed down  $\langle 100 \rangle$  directions in the 8-site  $\text{KNbO}_3$  model. A splitting of the atomic positions due to correlated atomic displacements is observed.

First, a combined fit of the neutron PDF and Bragg profile was performed starting from the ideal lattice sites. The fit produced discernable negative correlations among the nearest-neighbor Nb and O displacements which were evident in the doublet structure of the first peak in the total PDF. Despite an excellent agreement between the target and calculated data, the magnitude of the Nb-O correlations was much smaller compared to the target value. More importantly, the refined configuration exhibited no Nb-Nb and O-O correlations but instead featured positive K-K correlations, which were absent in the target model. No noticeable correlations existed beyond 4 Å. Clearly, the local structure obtained using powder total scattering data alone is grossly incorrect even though the 8-site and 2-site splitting was reproduced to some extent for the Nb and O probability density distribution functions, respectively. The fit also produced reasonable agreement between the calculated and target variances  $\langle u^2 \rangle$  for all the atomic positions. Unquestionably, without a prior knowledge of the structural, an incorrect model would have been inferred from RMC refinements using the neutron total scattering data.

In the second attempt, the neutron PDF and Bragg profile were complemented by the two electron diffraction patterns containing diffuse scattering. The results of a simultaneous fit of these four datasets are presented in Figure A4.2.

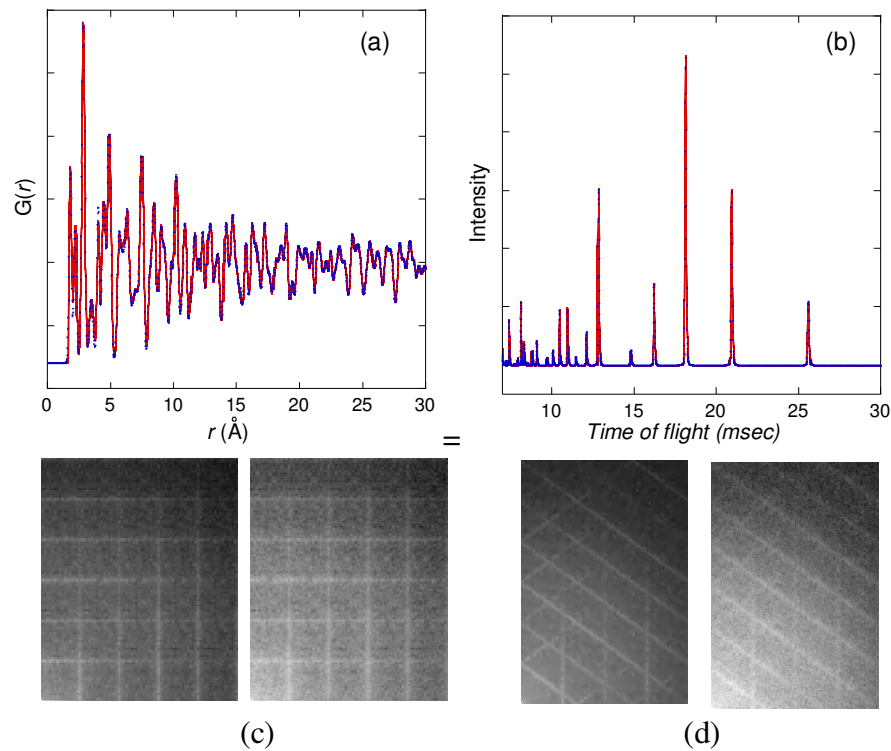


Figure A4.2: Results of a simultaneous fit of the neutron PDF and Bragg profile and electron diffuse scattering (two sections). (a, b) Experimental (blue) and calculated (red) neutron PDF (a) and Bragg profile (b). Experimental (left) and calculated (right) electron diffuse scattering patterns in the (130) (c) and (114) (d) sections of reciprocal space.

Now, the displacement correlations were reproduced in the refined configuration, although the correlation strengths were still significantly weaker than the target values. In particular, positive Nb-Nb and O-O displacement correlations were recovered and the incorrect K-K correlations, while still present, decreased considerably. Clearly, including the information encoded in electron diffraction improved considerably a correctness of the recovered displacement correlations.

#### A5. Algorithm for removal of incoherent scattering from neutron $S(Q)$

Strong incoherent neutron scattering that arises for example in samples containing hydrogen (H) has to be subtracted from the data to obtain a properly normalized  $S(Q)$ . Here we implemented a robust procedure for subtracting this incoherent background from the experimental data using RMCProfile and utility **Incoh\_subtr.exe**. This utility program first calculates the difference between the experimental  $S_{\text{exp}}(Q)$  and the  $S_{\text{calc}}(Q)$  calculated using RMCProfile for an atomic configuration representing the average structure with random atomic displacements and, then, fits this difference using an empirical 5-parameter analytical function  $f(Q)=Ae^{-BQ}Q^C+F/[(Q-D)^2+E^2]$ , where A, B, C, D, and E are adjustable parameters. The analytical expression was selected over a polynomial or a B-spline (also tried) because it does not introduce any oscillations of the kind that may arise due to real structural correlations. This fitted baseline function, represents a contribution of incoherent scattering as well as all other additive corrections that need to be subtracted from the data to obtain the correct shape for the sample background function. The correction is subtracted from the experimental data (using the external correction file option in PDFGetN) for each bank and the banks are merged.

The procedure involves the following steps:

1. Create an atomic configuration based upon atomic positions in the average structure using utility tools supplied with RMCProfile.
2. Displace the atoms in this configuration according to random Gaussian distributions with variances corresponding to atomic displacement parameters (ADP) in the average structure; these ADP parameters can be either adopted from Rietveld refinement or assigned arbitrary but sensible values. A utility such as supplied as a part of WinNFLP suite can be used to introduce random Gaussian displacements.
3. Obtain experimental  $S_{\text{exp}}(Q)$  for each detector bank using PDFGetN. Use any suitable spreadsheet software to convert these  $S_{\text{exp}}(Q)$  to  $F_{\text{exp}}(Q)$  according to  $F_{\text{exp}}(Q)=\langle b \rangle^2(S_{\text{exp}}(Q)-1)$ , where  $\langle b \rangle$  is the mean scattering length for the structure.
4. Prepare the RMCProfile \*.dat file and run RMCProfile to fit  $F_{\text{exp}}(Q)$  (as the experimental data) saving the results and stopping the run after a few cycles. Note that a baseline in the calculated  $S(Q)$  represents a realistic shape of the background for uncorrelated atomic motion.
5. Convert the output file \*\_SQ1.csv into the txt format and store in a folder with the **Incoh\_subtr.exe** utility.
6. Run **Incoh\_subtr.exe** and follow the on-screen instructions. The output file \*.fix is the background correction file for a given bank.
7. Use any spreadsheet software to combine the individual bank\*.fix files into a single .fix file that can be plugged into PDFGetN as an “external correction file”.

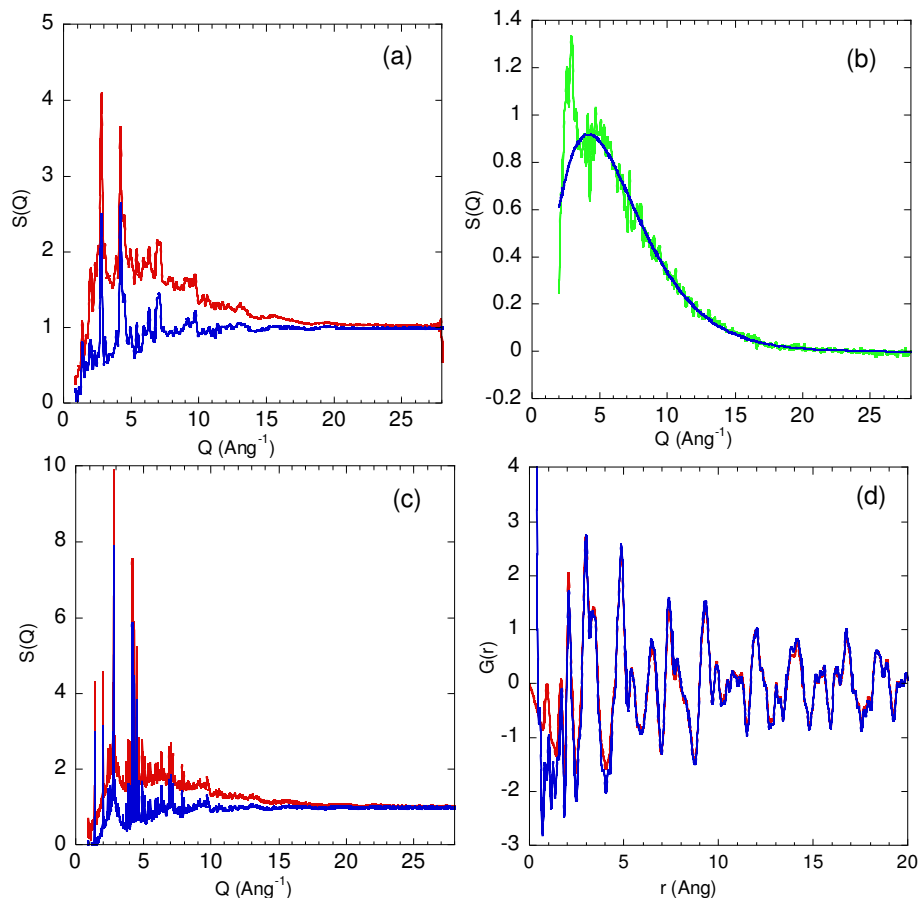


Figure A5.1: (a) Experimental (red) and calculated (blue)  $S(Q)$  for the  $\text{TiZrNiD}_2$  alloy. The experimental data were collected using the NPDF instrument. A limited D-H exchange reaction was sufficient to induce a significant background due to the incoherent scattering of H in the experimental data. The calculated  $S(Q)$  was obtained using RMCProfile for a configuration based on the Rietveld-derived model. The baseline in the calculated  $S(Q)$  provides a background expected for coherent scattering. (b)  $S(Q)$  for one of the detector banks having its baseline fitted using an analytical function  $f(Q)$  described in the text. (c)  $S(Q)$  before (red) and after (blue) subtraction of  $f(Q)$ . (d)  $G(r)$  obtained from  $S(Q)$  before (red) and after (blue) subtraction of incoherent scattering. Note the changes in the low- $r$  range. For  $r > 2 \text{ \AA}$ , the effect of incoherent scattering is rather insignificant.